



Universiteit  
Leiden  
The Netherlands

## Identifying Brain Network Topology Changes in Task Processes and Psychiatric Disorders

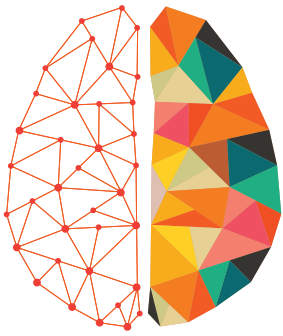
Rezaeinia, P.; Fairley, K.; Pal, P.; Meyer, F.G.; McKell Carter, R.

### Citation

Rezaeinia, P., Fairley, K., Pal, P., Meyer, F. G., & McKell Carter, R. (2020). Identifying Brain Network Topology Changes in Task Processes and Psychiatric Disorders. *Network Neuroscience*, 4(1), 257-273. doi:10.1162/netn\_a\_00122

Version: Publisher's Version  
License: [Creative Commons CC BY 4.0 license](#)  
Downloaded from: <https://hdl.handle.net/1887/137972>

**Note:** To cite this publication please use the final published version (if applicable).



# NETWORK NEURO SCIENCE

an open access  journal



Check for  
updates

Citation: Rezaeinia, P., Fairley, K., Pal, P., Meyer, F. G., & Carter, R. M. (2020). Identifying brain network topology changes in task processes and psychiatric disorders. *Network Neuroscience*, 4(1), 257–273. [https://doi.org/10.1162/netn\\_a\\_00122](https://doi.org/10.1162/netn_a_00122)

DOI:  
[https://doi.org/10.1162/netn\\_a\\_00122](https://doi.org/10.1162/netn_a_00122)

Supporting Information:  
[https://doi.org/10.1162/netn\\_a\\_00122](https://doi.org/10.1162/netn_a_00122)  
[https://github.com/SNaGLab/Rezaeinia\\_et\\_al\\_Hitting\\_time\\_analysis](https://github.com/SNaGLab/Rezaeinia_et_al_Hitting_time_analysis)

Received: 17 April 2019  
Accepted: 11 December 2019

Competing Interests: The authors have declared that no competing interests exist.

Corresponding Author:  
R. McKell Carter  
[mckellcarter@gmail.com](mailto:mckellcarter@gmail.com)

Handling Editor:  
Alex Fornito

Copyright: © 2019  
Massachusetts Institute of Technology  
Published under a Creative Commons  
Attribution 4.0 International  
(CC BY 4.0) license



## RESEARCH

# Identifying brain network topology changes in task processes and psychiatric disorders

Paria Rezaeinia<sup>1</sup>, Kim Fairley<sup>2,3</sup>, Piya Pal<sup>1</sup>, François G. Meyer<sup>4</sup>, and R. McKell Carter<sup>1,3,5,6</sup>

<sup>1</sup>Department of Electrical and Computer Engineering, University of California San Diego, San Diego, CA, USA

<sup>2</sup>Department of Economics, Leiden University, Leiden, The Netherlands

<sup>3</sup>Institute of Cognitive Science, University of Colorado Boulder, Boulder, CO, USA

<sup>4</sup>Department of Applied Mathematics, University of Colorado Boulder, Boulder, CO, USA

<sup>5</sup>Department of Electrical, Computer and Energy Engineering, University of Colorado Boulder, Boulder, CO, USA

<sup>6</sup>Department of Psychology and Neuroscience, University of Colorado Boulder, Boulder, CO, USA

**Keywords:** fMRI, Functional Connectivity, Random walk, Hitting time

## ABSTRACT

A central goal in neuroscience is to understand how dynamic networks of neural activity produce effective representations of the world. Advances in the theory of graph measures raise the possibility of elucidating network topologies central to the construction of these representations. We leverage a result from the description of lollipop graphs to identify an iconic network topology in functional magnetic resonance imaging data and characterize changes to those networks during task performance and in populations diagnosed with psychiatric disorders. During task performance, we find that task-relevant subnetworks change topology, becoming more integrated by increasing connectivity throughout cortex. Analysis of resting state connectivity in clinical populations shows a similar pattern of subnetwork topology changes; resting scans becoming less default-like with more integrated sensory paths. The study of brain network topologies and their relationship to cognitive models of information processing raises new opportunities for understanding brain function and its disorders.

## AUTHOR SUMMARY

Our mental lives are made up of a series of predictions about the world calculated by our brains. The calculations that produce these predictions are a result of how areas in our brain interact. Measures based on graph representations can make it clear what information can be combined and therefore help us better understand the computations the brain is performing. We make use of cutting-edge techniques that overcome a number of previous limitations to identify specific shapes in the functional brain network. These shapes are similar to hierarchical processing streams that play a fundamental role in cognitive neuroscience. The importance of these structures and the technique is highlighted by how they change under different task constraints and in individuals diagnosed with psychiatric disorders.

## INTRODUCTION

How do we link dynamic changes in functional brain structure to the processing of information? Brain activity organizes into stable networks that vary in strength and change with task demands (Greicius, Krasnow, Reiss, & Menon, 2003; Smith et al., 2009). Because of its ease of implementation and relatively low cost, the analysis of resting functional magnetic resonance imaging (rfMRI) data (Raichle et al., 2001) in particular has had a tremendous impact, leading

**fMRI:**  
Functional Magnetic Resonance Imaging: A resonance imaging technique used to detect blood oxygen levels changes in the brain, used as an aggregate measure of neural activity in the imaged region.

**Functional connectivity:**  
A measure of the functional relationship between two regions of the brain, generally via a measure of similarity between time courses from those regions.

**Random walk on graph:**  
A walk on the graph, which at each node selects the next node randomly from the connected nodes until reaching the destination.

**Lollipop graph:**  
A graph consisting of a complete component connected to a path graph (a linear chain of nodes).

**Resting state:**  
An experimental manipulation in which the subject is resting and is not actively engaging in a task.

**Adjacency matrix:**  
A matrix representation of a graph with  $i_j^{th}$  element indicating the weight of the edge from node  $i$  to node  $j$ .

to several large-scale public initiatives like the Human Connectome Project (HCP; Essen et al., 2013). One of the most promising methods used to study fMRI activation has been to construct network models of functional connectivity between areas of the brain (E. T. Bullmore & Bassett, 2011; Goñi et al., 2014; van den Heuvel & Pol, 2010). These models are characterized by network measures like efficiency (Fornito, 2016) and have been applied to a wide variety of challenges including the study of psychiatric disorders (for review, see Avena-Koenigsberger, Misisic, & Sporns, 2017). Improving our ability to interpret the meaning of these measures for brain processing would have tremendous impact.

To improve our ability to interpret network models of brain connectivity, we seek measures of topology that can be related to models of cognitive information processing. The study of the relationship between brain network topology and function has been accelerating and is key to explaining dynamic information processing in health and disease (Stiso & Bassett, 2018). To better understand how information is processed in a dynamic context, it is necessary to link specific brain-network topologies to cognitively meaningful information-processing structures. Network analysis of brain data typically involves descriptions of an inferred network. Here, we instead describe brain connections as stochastic processes (in our case, using a random walk), avoiding the constraints of a specific network model and instead describing general properties of brain functional connectivity in a given mental state. This improved description of brain connectivity can then be used to link results from graph theory to network topologies common in cognitive models of the brain. As a first step, we utilize a result from the theory of graph measures, which establishes that isolated chains of nodes produce maximally long random walks between points on the graph. In particular, a lollipop graph consists of a set of fully connected nodes attached to a chain of linearly connected nodes. In a random walk on a lollipop graph, the number of hops required to reach the tail of the lollipop stick is greater than for other topological structures (Brightwell & Winkler, 1990). We target extremely long random walks between brain areas as a measure of the presence, and relative isolation, of linear chains of nodes. We note that this topology is similar to that found in hierarchical processing streams, a structure important in cognitive models. We hypothesize that those brain areas that take a long time to reach in a random walk are often situated in such an information-processing topology.

We focus on the tails of random-walk network connectivity distributions to address the following four key questions. (a) How does the relative isolation of a linear chain of nodes change the distribution of connectivity in a synthetic network? (b) Are there subnetworks in resting-state cortex that have properties similar to a linear chain of nodes? (c) How are linear-chain subnetworks changed by task demands? (d) Does the characterization of network topology have value in understanding and diagnosing psychiatric disorders?

## **MATERIALS AND METHODS**

### ***Hitting-Time Functional Connectivity Model***

One common approach to find the connectivity matrix of a brain network is to threshold the Pearson correlation matrix to obtain the adjacency matrix for the network. Although this method is very simple, it has some shortcomings that might cause inaccuracy in the results. One challenge is that the Pearson correlation coefficient does not account for latent variables, which might result in a high correlation among two regions that are not directly connected. In addition, the choice of threshold is arbitrary, creating interpretation and generalization issues. To overcome these challenges, we integrated the following changes into a standard network analysis pipeline for neuroimaging. First, to compensate for latent variables, we use the partial

Partial correlation:

Linear correlation of two variables controlling for the effect of other variables in the model.

Hitting time:

The expected number of hops to go from one node to another node by running a random walk on the graph.

Probability transition matrix:

A matrix representation of a graph with  $ij^{th}$  element representing the probability of transitioning from node  $i$  to node  $j$ .

correlation (Smith et al., 2011) to find the connectivity matrix. Let  $\rho_{ij}$  represent the partial correlation between  $x_i$  and  $x_j$  (the BOLD time series associated with regions  $i$  and  $j$ , respectively). Therefore, we use a weighted brain functional network with adjacency matrix  $A = [\rho_{ij}]$ . The degree of node  $i$  is  $d_i = \sum_{j=1}^N |\rho_{ij}|$ . Second, we normalize edge strength using self loops that preserve the overall connectivity of each node relative to others. Third, we characterize the network using the hitting time, a random-walk measure that reflects the expected number of edges that need to be crossed to transition from one node to another. We next describe the edge strength and hitting-time approaches in detail.

**Edge Strength Normalization**

For a random walk, the probability transition matrix is  $P = [p_{ij}]$ , where  $p_{ij}$  is defined as

$$p_{ij} = \frac{|\rho_{ij}|}{\sum_{j=1}^N |\rho_{ij}|} = \frac{|\rho_{ij}|}{d_i}. \tag{1}$$

The major drawback of this definition is that it fails to distinguish a strongly connected from a weakly connected node. Consider a network with five nodes (a, b, c, d, e) and six edges. Suppose that all edges connected to node a have weight 0.9. And, suppose that node b is connected to the same nodes as node a, but with edges with weight 0.1 (Figure 1A). Applying Equation 1, both nodes a and b will have the same transition probabilities, and therefore, the same relative connectivity.

To overcome this problem, we add a self loop to nodes with weaker connections. To implement this, we find the node with maximum degree in the network. For every other node, we subtract the degree of that node from the maximum degree and add that as a self edge to the node. Therefore, the new degree matrix is  $D' = d_{max}I$ , and the new adjacency matrix is  $A' = [\rho'_{ij}]$ , where

$$\begin{aligned} \rho'_{ij} &= \rho_{ij}, & i, j = 1, \dots, N \text{ and } i \neq j, \\ \rho'_{ii} &= d_{max} - d_i, & i = 1, \dots, N, \end{aligned} \tag{2}$$

$$d_{max} = \max_i(d_i), i = 1, \dots, N, \text{ and } I \text{ is the identity matrix.}$$

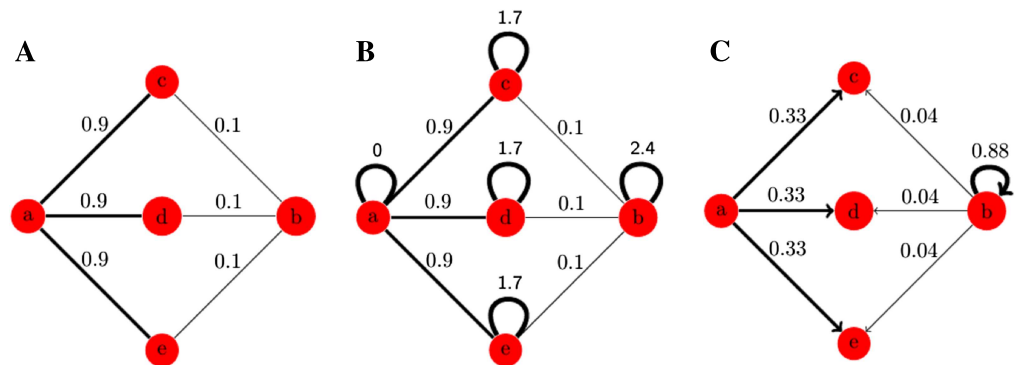


**Figure 1.** Edge strength normalization to maintain connectivity differences between a strongly connected and a weakly connected node. (A) A weighted graph with five nodes and six edges. (B) Adding self loops to nodes with weaker connections in order to normalize the probabilities. (C) Transition probabilities from nodes a and b after normalization (the transition probabilities from nodes c, d, and e are not included in this figure).

### Hitting Time

We run random-walk models on the graph with the new transition probability matrix  $P' = D'^{-1}A'$  to calculate the hitting-time matrix  $H = [h_{ij}]$ . The hitting time from node  $i$  to node  $j$ ,  $h_{ij}$ , is the expected number of hops to visit node  $j$  for the first time, for a random walk started at node  $i$ .

Hitting time is an asymmetric measure, meaning that  $h_{ij}$  and  $h_{ji}$  might be different. For example, for a lollipop graph, the hitting times from the nodes on the complete component to nodes on the chain are much larger than the reverse direction, because a random walker spends more time in the complete component. We compute the hitting times between pairs of nodes using the graph Laplacian method introduced in spectral graph theory (Aldous & Fill, 2002). This method is advantageous as it does not require the exact knowledge of the adjacency matrix, instead using a probabilistic approximation of the adjacency matrix of the network. Following Lovász and Simonovits (1993), we calculated the normalized graph Laplacian as

$$\mathcal{L} = D'^{-1/2}(D' - A')D'^{-1/2} = I - P', \quad (3)$$

where,  $D'$  is the degree matrix and  $A'$  is the adjacency matrix of the graph after normalization as defined in the main text. We used the eigenvalues and eigenvectors of  $\mathcal{L}$  to calculate the hitting-time matrix  $H = [h_{ij}]$  (Lovász & Simonovits, 1993);

$$h_{ij} = \sum_{k>1} \frac{d'}{\lambda_k} \left( \frac{\mu_{kj}^2}{d'_j} - \frac{\mu_{ki}\mu_{kj}}{\sqrt{d'_i d'_j}} \right), \quad i, j = 1, \dots, N \text{ and } i \neq j, \quad (4)$$

$$h_{ii} = 0, \quad i = 1, \dots, N,$$

where,  $d'_i$  is the degree of node  $i$ ,  $i = 1, \dots, N$ , and  $d'$  is the sum of all degrees (after normalization; see main text).  $0 = \lambda_1 < \lambda_2 < \dots < \lambda_n$  are the  $n$  eigenvalues of  $\mathcal{L}$ , and  $\mu_{kj}$  is the  $j$ th element of  $k$ th eigenvector of  $\mathcal{L}$  (Lovász & Simonovits, 1993).

Adding the self loops in the normalization step does not make the graphs reducible or periodic, meeting the requirements of the hitting-time calculation we use here (Norris, 1997). Code for analysis in this project can be found under the first author's name on GitHub: <https://github.com/SNaGLab: Hitting-time-analysis> (Rezaeinia, 2018).

## RESULTS

To detect and characterize linear chains of nodes, we focus on the random-walk measure of connectivity hitting time (Lovász & Simonovits, 1993) defined above. In synthetic graphs and estimated networks, a node is a point in the graph (or area of the brain) and an edge is a connection between two nodes. Hitting time between nodes  $i$  and  $j$  is a random variable describing the number of steps to get from node  $i$  to node  $j$  for the first time (represented as  $h_{ij}$ ) during a random walk, a measure equivalent to mean first-passage time (Avena-Koenigsberger et al., 2017). Diffusion measures of networks, like hitting time, are becoming more commonly used and are the focus of active research (Goñi et al., 2013; Lambiotte, Delvenne, & Barahona, 2014; Shen & Meyer, 2008). Diffusion-based measures carry significant methodological advantages. First, they overcome common issues caused when thresholding is used to define binary connections (Goulas, Schaefer, & Margulies, 2015; Reijneveld, Ponten, Berendse, & Stam, 2007; Rubinov & Sporns, 2011; Zalesky, Fornito, & Bullmore, 2010). Second, they do

Graph Laplacian:  
A matrix representation of a graph, which can be used to extract various properties of the graph.

not require perfect knowledge of the network to make a robust estimation of connectivity (i.e., it does not require the exact adjacency matrix (Lovász & Simonovits, 1993). Third, measures like hitting time are asymmetric, meaning hitting time from one node to another may be different from the return trip, giving the best opportunity to identify extremeness in connectivity (Lovász & Simonovits, 1993). Here, we will use “hitting time” to refer to the expected number of edges to be traversed rather than the variable itself and “hitting-time distribution” to be the subject-average distribution of the expected number of edges to be traversed when moving between combinations of nodes. We begin by looking at the relationship between extreme hitting times and synthetic graph structure and then extend those findings to a publicly available functional magnetic resonance imaging (fMRI) dataset.

**How does the relative isolation of a linear chain of nodes change the distribution of connectivity in a synthetic network?** We consider a chain of sequentially connected nodes as a model for a hierarchical processing stream. Formally, a chain of sequentially connected nodes can be described as  $N$  nodes arranged in a line, so that there is an edge between nodes  $i$  and  $i + 1$  for  $i = 1, \dots, N - 1$ , and no edges between nodes  $i$  and  $j$  where  $j \neq i - 1, i + 1$ . Theoretical results have found that a chain of sequentially connected nodes attached to a fully connected network (i.e., a lollipop graph) results in maximal hitting times when the chain is a third of the network (Brightwell & Winkler, 1990). We now compare the distribution of hitting times over nodes in a lollipop graph to small-world (Watts and Strogatz, 1998), random (Erdős-Rényi; Erdős and Rényi, 1959), and complete synthetic graphs in Figure 2. Each graph consists of 100 nodes. Random and small-world graphs are an average of 100 configurations. Linear

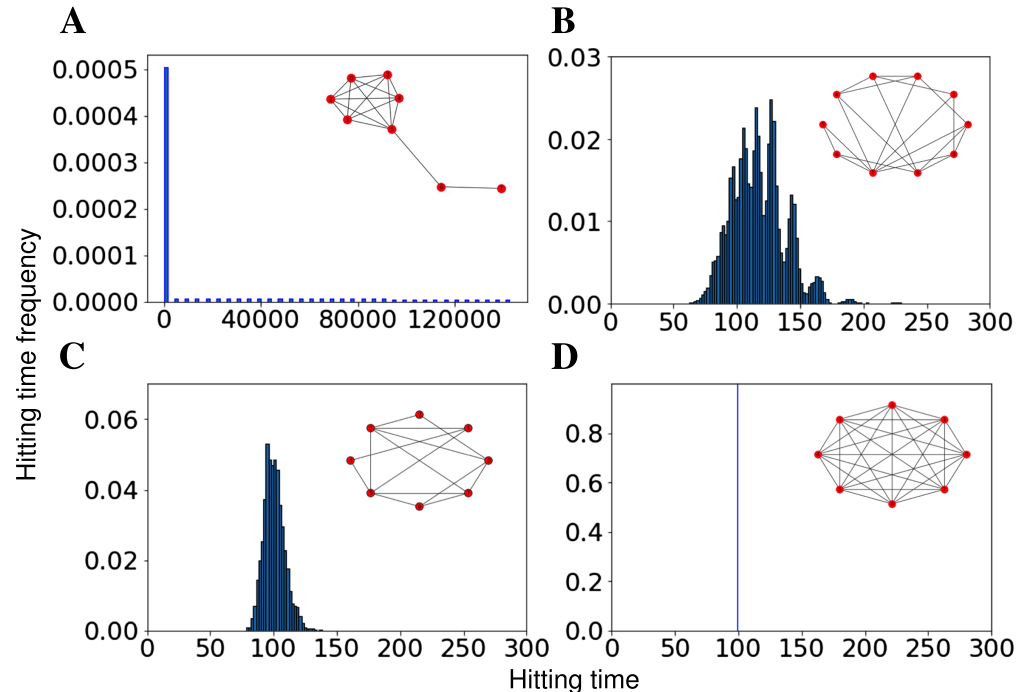


**Figure 2.** Hierarchical processing streams in lollipop graphs produce extremely long hitting times. Hitting-time distributions for (A) lollipop, (B) small world, (C) random, and (D) complete graphs with 100 nodes (averaged over 100 runs for small-world and random networks). The graphs on top of the distributions are smaller representations of the graphs used to generate the distributions. Axis scales change significantly with graph type (e.g., lollipop hitting time is several orders of magnitude larger than the other graphs).



Kelley skewness:  
A percentile based measure of skewness defined as  $P_{90} + P_{10} - 2 \times P_{50}$ .

chains of nodes result in larger hitting times that produce increased skewness in the hitting-time distribution. For example, in Figure 2, panels A and D represent two extreme examples of hitting-time distribution in a network. Because of the presence of a path in A, the hitting time has a long tail (nonzero probability) that extends to large values (above 120,000). While in D each node is fully connected to every other node and hence, hitting time is the same across all pairs (in this case, 100) and the distribution is a single value with no tail. We focus on Kelley skewness (Kelley, 1923) as our measure of skewness because it directly compares the tails of the distribution. Kelley skewness (hereafter just skewness) therefore provides a more robust separation of extreme cases from changes in the interior of the distribution.

Although perfectly isolated linear chains of nodes produce extreme hitting times, it is possible that even weak connections to the chain might significantly reduce hitting times to nodes on the chain. To characterize changes in the hitting-time distribution when a linear chain of nodes is not perfectly isolated, we begin with a random graph and alter its connectivity to isolate a linear chain of nodes (Figure 3). Beginning with 50 nodes, edges of weight 1 were added between each pair of nodes with a probability of 0.6. We then randomly chose 10 connected nodes in the graph (1/5 of the graph) and reduced the weight of edges between those connected nodes and the rest of the network by 0.05 for 19 iterations. This process created a linear subgraph that becomes progressively more isolated until it resembles the stick of a lollipop graph. As a control for reduced connectivity across the network as a whole, we took the same graph we started with above and reduced all existing edge weights by 0.05 for 19 iterations. To preserve the reduction in overall connectivity (edge weights are typically normalized by the total connectivity of a node), edge weight reductions were added back as self loops (see Materials and Methods). These self loops are required as part of the random walk to preserve the physiological principle that reduced neuronal activity would result in a reduction of connectivity (not just a shift between connections).

Average hitting time increases as the chain of nodes becomes more isolated but also when the graph becomes more disconnected as a whole. Hence, mean hitting time does not distinguish between these two scenarios. However, in our simulations, skewness changed

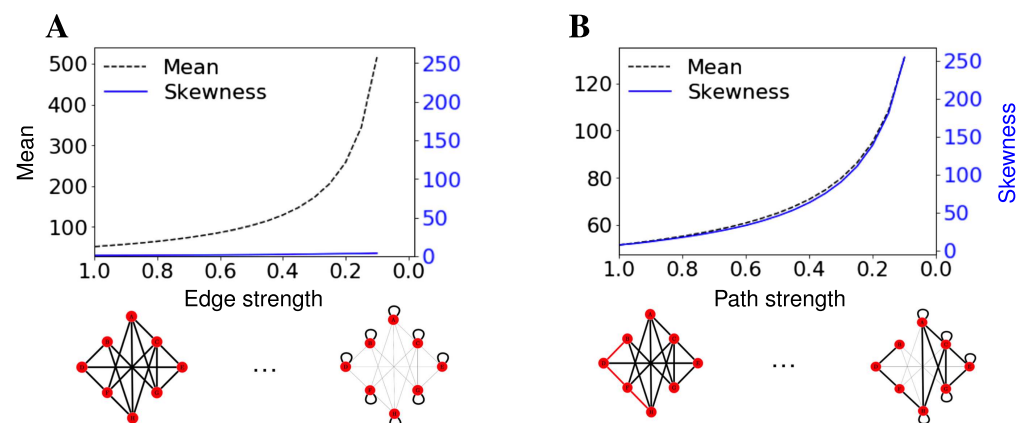


**Figure 3.** The skewness of the hitting-time distribution distinguishes a reduction of overall connectivity from a subgraph that becomes more linear. (A) Mean and skewness of hitting-time distribution as the strength of all connections is reduced by 0.05 for 19 iterations. Toy networks for this transition are represented on the x-axis. Reductions in connectivity are added as self loops. (B) Mean and skewness of hitting-time distribution as the strength of connections between linear component and the rest of the graph is reduced by 0.05 for 19 iterations. Toy networks on the x-axis represent synthetic graphs with a linear subgraph as the path (red) is made more linear.

significantly as the linear subgraph becomes more isolated but only minimally when the average connectivity of the whole graph decreased. Skewness also increased with the relative isolation of the chain of nodes but was present even when each node in the chain was somewhat connected to the rest of the graph (Figure 3).

We have shown that a lollipop component present in a graph results in significant increase of (Kelley) skewness of hitting-time distribution, but is this relationship true in heterogeneous topologies? It is important to note that other changes in graph structure may also result in extreme hitting times. One commonly employed graph measure is modularity, the extent to which the graph can be easily separated into different communities.

To evaluate the effect of modularity on hitting-time distribution, we have tested a large number of networks with different levels of Louvain modularity and numbers of chain motifs (three node linear components). We generated random networks, each with 100 nodes varying the number of edges. To allow a comparison across a given number of edges, we generated multiple graphs with the same number of edges by choosing  $k$  edges uniformly from the full possible set of edges.  $k$  was varied from 200 to 1,000 in intervals of 50 and 1,000 to 2,500 in intervals of 100. The range of the average degree is [4, 50], with a range of Louvain modularity of [0.1, 0.6]. Keeping only those graphs that were connected resulted in 15,243 graphs for comparison. Using a linear model, we sought to explain skewness as a function of modularity, number of edges, and number of chain motifs. Number of edges ( $p < 0.001, t(15,241) = 4.16, \beta = -0.0052$ ), modularity ( $p < 0.001, t(15,241) = 37.4, \beta = 239$ ), and the number of chain motifs ( $p < 0.001, t(15,241) = 13.8, \beta = 9.5$ ) all independently explain some variance in skewness. In the remaining analysis of brain networks, we therefore test whether nodes with extreme hitting times also become less chain-like.

**Are there subnetworks in resting-state cortex that have properties similar to a linear chain of nodes?** Motivated by the above simulations, we utilized the skewness of the hitting-time distribution to identify potential linear chains of nodes in cortical connectivity data. The brain is made up of a large number of highly interconnected regions (Cherniak, 1990) evolved to efficiently integrate a variety of sources of information (Friston, 2010) that can be represented as a network. Graph-theoretic models of the brain have been used to effectively segment commonly associated regions of the brain into large-scale networks and describe the properties of brain information processing (for review see E. Bullmore & Sporns, 2009) in health and disorder (Bassett & Sporns, 2017; Fox & Greicius, 2010). Characterizations of brain network changes in development or psychiatric disorder often utilize graph measures like efficiency (Latora & Marchiori, 2001) and small-worldness (Watts & Strogatz, 1998), which typically include the average path length in their definition (for common measurement descriptions, see Achard & Bullmore, 2007). Even measures that may not directly utilize the average path length (e.g., modularity, Newman & Girvan, 2004; Stiso & Bassett, 2018) sometimes rely on community detection methods that incorporate the average path length. The use of an average path length rests on the assumption that path lengths in that network are normally distributed and so can lead to the mischaracterization of the topology of the network. The concern arises because of the use of an average and is present in both traditional and diffusion-based graph measures. Overcoming this assumption requires the use of specific subnetwork models (for example, see Khambhati, Medaglia, Karuza, Thompson-Schill, & Bassett, 2018) or the capture of deviations from normality in the path-length distribution. Here, we use Kelley skewness of the hitting-time distribution to distinguish changes in the network as a whole from the presence of network topologies resembling hierarchical processing streams.



To test for the presence of skewness in cortical connectivity, we generated a hitting-time measure of connectivity (see Materials and Methods) for resting-state functional data from neurotypical participants who were part of a large open-source dataset (LA5c, UCLA Consortium for Neuropsychiatric Phenomics; Poldrack et al., 2016; see Supporting Information). Network nodes were 180 anatomical regions from the multimodal parcellation of Glasser et al. (2016). The average hitting-time distribution of neurotypical resting-state functional connectivity is positively skewed (Kelley skewness of 15.04 and Pearson's coefficient of skewness of 2.3); see Figure 4A. A D'Agostino-Pearson test (Trujillo-Ortiz & Hernandez-Walls, 2003) showed that as a whole the hitting times were not normally distributed ( $Z(\text{skew}) = 110,3496, \chi^2(2) = 17,864.8071, p < 0.001$ ).

Although skewness of a distribution can originate from many sources, ranging from a smooth shift of the distribution as a whole to far-ranging outliers, the particular skewness measure used here (Kelley skewness) directly compares the extremes of the distribution (90% compared with 10%), limiting the potential causes of the skewness. Limiting our test for skewness to the tails of the distribution is consistent with our aim of identifying changes in linear-chain topologies, which have been shown to produce maximal hitting times in lollipop networks (see above). The primary auditory, visual, and somatosensory hierarchies show the largest average to-hitting times (Figure 4B), and are therefore possibly related to chain-like network topologies. It is important to note that even the use of a Kelley skewness metric does not guarantee the presence of chain-like network topologies. In fact, random graphs generated from a stochastic block model that precluded chain-like topologies exhibited Kelley skewness explained by modularity and node degree. We generated 100 graphs with 180 nodes from a stochastic block model. To define groups and mixing structure, we fixed the probability of connections within communities to be ( $p = 0.7$ ) and between communities to be ( $q = 0.1$ ). To expand the range of possible modularity, we randomly picked the number of nodes in each community until we reach 180 (if the total number of nodes passes 180, we reduce the size of the last community to have a total of 180 nodes in the graph). After removing the null values, we ended up with 89 graphs with number of communities from 2 to 6 and Louvain modularity

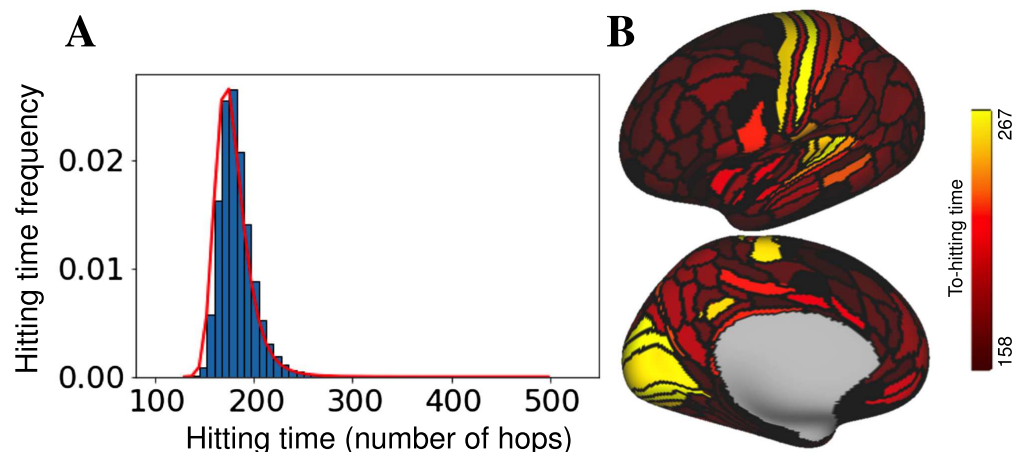


**Figure 4.** Hitting-time measures of resting-state functional connectivity in neurotypical participants are positively skewed. (A) Average normalized hitting-time distribution for control subjects during resting state from the publicly available LA5c study. (B) Average to-hitting time from all other regions of cortex for lateral (top) and medial (bottom) left maps thresholded to [158(10%), 267(95%)]. The range of data is [129, 310]. Primary auditory, visual, and somatosensory cortices have the largest to-hitting times in the cortex.

levels of 0.03 to 0.42. These Stochastic block model networks contain Kelley skewness that is explained by both modularity ( $\beta = -1.591e + 03, t(86) = -10.76, p < 0.001$ ) and degree ( $\beta = -8.617e - 02, t(86) = -7.39, p < 0.001$ ). Because Kelley skewness may arise from multiple sources, we next look for changes in the skewness of the hitting-time distribution during a task and ask whether those changes are related to regions of the brain with the largest hitting times during resting scans, and then, whether those areas with the largest rest hitting times also become less chain-like.

**BART:**  
Balloon Analogue Risk Task is a paradigm designed to study risk taking in an experimental setting.

**How are linear-chain subnetworks changed by task demands?** To better interpret the skewness of cortical networks during resting-state fMRI, we sought to test whether hitting times become more or less skewed during task performance and which connectivity changes underlie those shifts. We compared resting-state and balloon analogue risk task (BART) functional connectivity from the LA5c study. The BART is a paradigm designed to study risk taking in an experimental setting. Participants in the BART decide whether to pump a balloon that is at risk of popping. The BART is defined by visual input and motor responses without structured auditory stimulation.

Hitting times between cortical areas were calculated for fMRI data collected during the performance of the BART task using the same processing pipeline as for the resting-state scans. To test for differences in skewness, we then ran a linear mixed-effect model (lme in R) of skewness of the hitting-time distributions (dependent variable) modeling task (with resting state as a reference), gender, and age as independent variables. The task variable was treated as a random effect (BART and resting-state points were paired by participant), which characterizes idiosyncratic variation that is due to individual differences. In our first model, we found significant difference in skewness for control subjects between BART and rest ( $\beta = -10.25, t(118) = 0.79, p < 0.001$ ); see Figure 5. The skewness of hitting-time distribution is significantly reduced in the BART ( $\mu = 5.48, \sigma = 3.96$ ) compared with rest ( $\mu = 15.73, \sigma = 8.49$ ). Age and gender did not significantly explain variance in this model. We next sought to test whether this skewness could be related to nodes with extreme hitting times and whether those nodes define network topologies that become less chain-like.

To identify those nodes related to differences between rest and task, we first ask which nodes had the largest hitting-time changes. The 10 regions with the largest hitting-time changes (paired  $t$  test comparing task and rest hitting times, significantly different with  $p < 0.05$ , Bonferroni corrected) are V2, V3, V4, V3A, and PGs within the visual cortex, 1, 4, 3b, and OP4 within somatosensory cortex, and the area 'PF'; see Figure 5B–D. Regions are labeled according to Glasser et al. (2016). These nodes, which show decreased hitting times during task performance, overlap heavily with the visual and motor processing streams and correspond to many of the nodes with the largest hitting times during rest scans. This reduction in hitting time in the visual and motor pathways during the BART provides support for the role of these pathways in skewness but does not address whether differences in the chain-like topology is responsible for the change in hitting times.

To add support for the role of chain-like topologies in large hitting times in brain data, we calculated a chain index for each node that provides a measure of how similar to an isolated chain the local connectivity of the node is. For every node in the network located on a three-node chain motif, we define a chain index by focusing on its two strongest connections. A node is located on a chain motif if its neighbors with the two strongest connections are stronger than the remaining connections and if the two strongest connections have a significantly weaker connection with each other. Assuming that node  $i$  is on a chain motif and has  $N_i$  neighbors

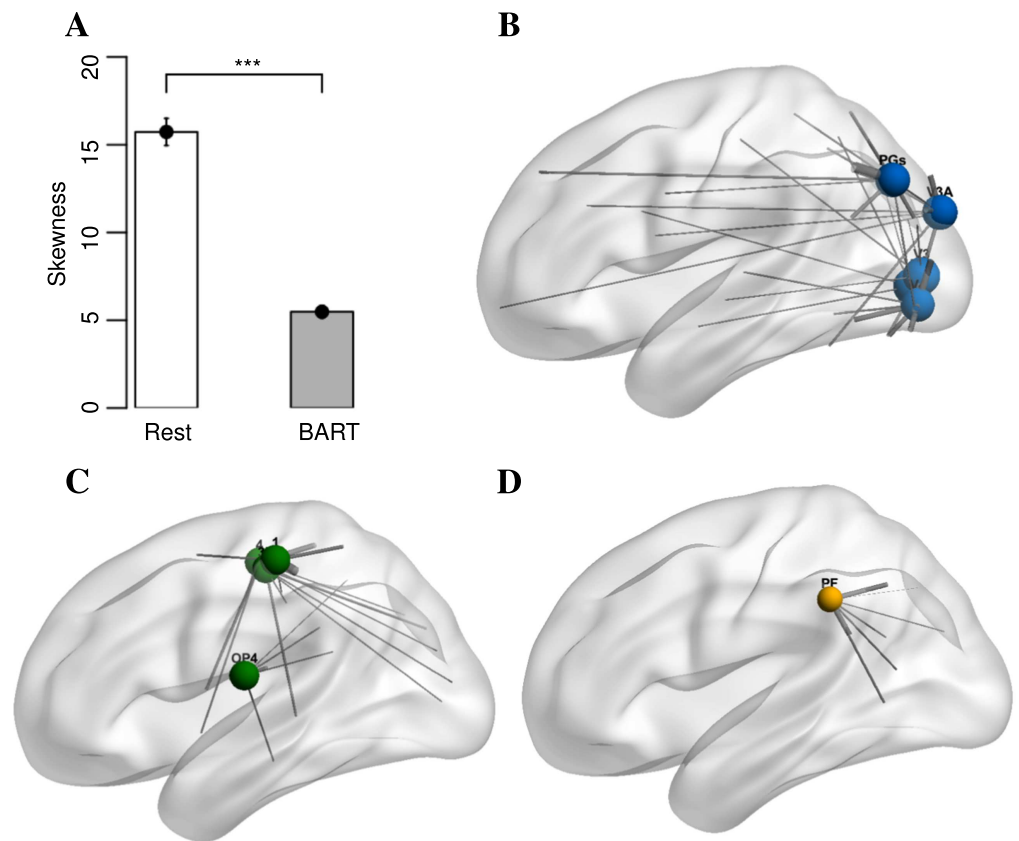


**Figure 5.** The distribution of skewness versus task for control subjects.  $p$  value significance codes:  $.$  = 0.1,  $*$   $\leq$  0.05,  $**$   $\leq$  0.01,  $***$   $\leq$  0.001. The skewness of hitting-time distribution for control subjects is significantly smaller when the subjects are engaged in BART task compared with rest. The 10 nodes with largest hitting-time changes are (B) V2, V3, V4, V3A, and PGs (visual), (C) 1, 4, 3b, and OP4 (motor), and (D) PF. The size of each node represents the magnitude of difference of average to-hitting times (range from 19 to 30.2) and the thickness of each edge represents the magnitude of difference of partial correlation in BART compared with rest.

and nodes  $i_1$  and  $i_2$  have the strongest connections to node  $i$ , we define chain index for node  $i$  as

$$\zeta_i = \rho_{ii_1} + \rho_{ii_2} - \sum_{j=3}^{N_i} \rho_{ii_j}.$$

If a node is located on a perfect chain, the chain index will be at its maximum. If a node has equal connections to every other node in the network (the least chain-like network), the chain index will be a large negative number that depends on the number of nodes in the network.

Comparing connectivity during the BART with rest, the largest reductions in the chain index were for a set of nodes that overlapped heavily with those nodes with the largest hitting time (8 of the 10 nodes described above), including V2, V3, V3A, V6, and V6A within the visual cortex, 1, 4, 3b, and OP4 within somatosensory cortex, and the area PF. Labels are according to Glasser et al. (2016). In accordance, the nodes with the largest hitting-time changes also show increased connectivity during the BART. Connections from nodes with the largest hitting times that have changed significantly (paired  $t$  tests comparing connections from each node during task and rest,  $p < 0.05$  Bonferroni corrected) are indicated in Figure 5 by gray lines,

with the thickness of the line indicating the size of the change. During task performance, nodes in task-related sensory streams (which have large hitting times during rest) have smaller hitting times, becoming less like isolated chains and instead more widely integrated.

**Does the characterization of network topology have value in understanding and diagnosing psychiatric disorders?** Brain network efficiency, which is commonly defined by the mean distance between nodes, has been shown to change in disorders such as Alzheimer's (Dennis & Thompson, 2014), schizophrenia (Besnard et al., 2018; Li et al., 2017), and others (Cheng et al., 2016). Reductions in measures of efficiency that utilize mean distance could be due to (a). Reduced overall connectivity; or (b) subnetwork changes that lead to skewed hitting-time distributions. As described in Figure 3, we can distinguish these possibilities by focusing on skewness. If skewness changes, the differences between psychiatric populations and controls is more likely to be due to subnetwork changes than a change in overall connectivity. We ran an ordinary least squares regression model with skewness of the resting-state hitting-time distribution as the dependent variable, and group (dummy coded, reference controls), gender (dummy coded, reference females), and age (mean centered, linear) as independent variables. We analyzed resting-state functional data from four patient groups, control, schizophrenia, bipolar, and attention deficit hyperactivity disorder (ADHD). We found significant differences in skewness between schizophrenia and control populations ( $\beta = -5.130, t(252) = 1.268, p < 0.001$ ), bipolar and control populations ( $\beta = -4.060, t(252) = 1.324, p < 0.001$ ), and a trend-level difference between ADHD patients and control populations ( $\beta = -2.445, t(252) = 1.324, p = 0.066$ ), see Figure 6. Gender and age did not significantly explain variance in this model.

To identify those nodes related to skewness differences between schizophrenia, bipolar disorder, and controls, we first ask which nodes had the largest hitting-time changes. The 10

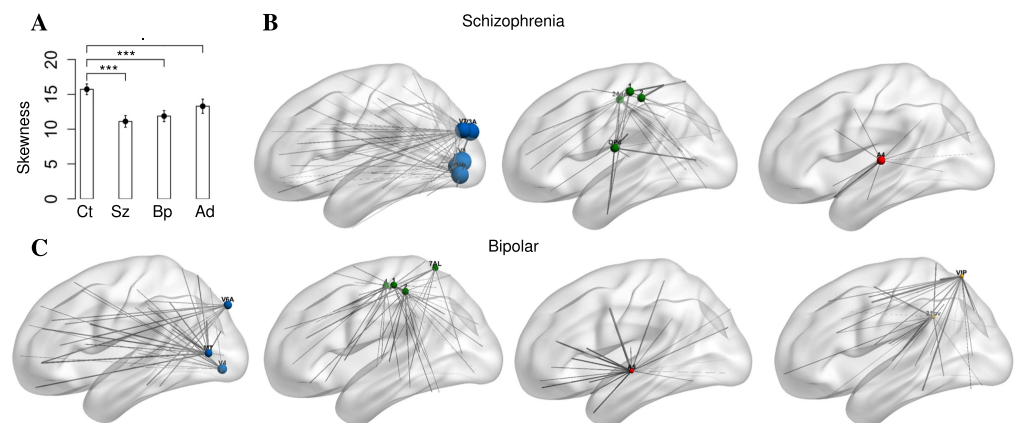


**Figure 6.** Skewness of the hitting-time distribution is significantly different across patient groups. (A) Distribution of skewness of the hitting-time distributions in patient and control groups during resting-state scans. Ct, Sz, Bp, and Ad stand for control, schizophrenia, bipolar, and ADHD, respectively. Significance codes: . = 0.1, \*  $\leq$  0.05, \*\*  $\leq$  0.01, \*\*\*  $\leq$  0.001. The skewness of hitting-time distribution is significantly smaller for subjects with schizophrenia and bipolar disorders compared with neurotypicals. The 10 nodes with the largest change in hitting time for subjects with schizophrenia include V2, V3, V4, V3A, and V7 (visual, top blue), 1, 2, 24dd, and 4 (motor, top green), and A4 (auditory, top red). The 10 nodes with the largest change in hitting time for subjects with bipolar disorder include MT, V4, and V6A (visual, bottom blue), 1, 2, 4, and 7AL (motor, bottom green), A5 (auditory, bottom red), and VIP and 31pv (bottom yellow). The size of each node represents the magnitude of difference of average to-hitting times (range from 7.1 to 33.4) and the thickness of each edge represents the magnitude of difference of partial correlation in psychiatric disorder compared with control subjects during rest.

regions with the largest hitting-time changes between (*t* tests comparing schizophrenia and control groups for each region, significantly different with  $p < 0.05$  Bonferroni corrected) were V2, V3, V4, V3A, and V7 within the visual cortex, 1, 2, 4, and 24dd within somatosensory cortex and A4 within the auditory cortex for subjects with schizophrenia. For subjects with bipolar disorder, the 10 regions with the largest hitting-time changes (significantly different in *t* tests comparing bipolar and control groups with  $p < 0.05$  Bonferroni corrected) were MT, V4, and V6A within visual cortex, 1, 2, 4, and 7AL within somatosensory cortex, A5 within auditory cortex, and VIP and 31pv. Regions are labeled according to Glasser et al. (2016). Connections that have changed significantly (*t* tests comparing connections from each node between groups,  $p < 0.05$  Bonferroni corrected) from these nodes are indicated by gray lines, with the thickness of the line indicating the size of the change.

We find evidence that individuals with schizophrenia and bipolar disorder have less skewed hitting-time distributions than controls during resting-state fMRI. The regions of cortex with the largest hitting-time reductions between patient and control populations are in sensory/motor cortex and overlap with many of the same regions that have extremely large to-hitting times during rest in controls. It is possible that the large hitting-time values found in these regions of the cortex are related to the theoretical finding that linear chains of nodes produce maximal hitting times and that a reduction in hitting time in these regions occurs when the nodes are part of a topology that is less chain-like. We therefore also compared the chain index for schizophrenia, bipolar, and control groups. The 10 regions with the largest changes of chain index (*t* tests comparing schizophrenia and control groups for each region, significantly different with  $p < 0.05$  Bonferroni corrected) are V2, V3, V4, V3A, and V7 within the visual cortex, 1, OP4, and 24dd within somatosensory cortex, and A4 and A5 within the auditory cortex for subjects with schizophrenia. For subjects with bipolar disorder, the 10 regions with the largest changes of chain index (significantly different in *t* tests comparing bipolar and control groups with  $p < 0.05$  Bonferroni corrected) are V4, V3A, and V6A within visual cortex, 1, 2, 4, and 7AL within somatosensory cortex, A5 within auditory cortex, and VIP and PFcm. The convergence of evidence of changes in extreme hitting-time values in sensory areas of cortex and those same areas being connected in a less chain-like topology in schizophrenia and bipolar disorder is consistent with our hypothesis that path-length changes in these populations are likely to be related to subnetwork topology shifts and not changes to the network on average.

## **DISCUSSION**

We have presented evidence that the skewness of connectivity in cortical brain networks can be used to infer likely network topology changes that improve our understanding of information processing in the brain. Using random graphs we showed that the isolation of linear motifs is one prominent cause of skewness in hitting time even in the presence of mixed topologies. We then showed that skewness, but not average of brain-connectivity distributions, is related to psychiatric diagnosis. We confirmed that these differences in skewness were related to a linear-chain topology by testing for changes in a chain index. In networks for which connectivity is positively skewed, a change in subnetwork topology (and possibly a different brain state) is a more parsimonious explanation than changes in average connectivity. These topology changes are focused in sensory areas of the brain, and when compared with changes brought about during task performance, they provide an initial mechanistic link between resting-state connectivity changes and clinical diagnosis.

Extremely large hitting times can be linked to linear-chain topologies through theoretical work showing that lollipop networks result in maximal hitting times (Brightwell & Winkler,



1990). We have shown using a toy problem that the extremeness of hitting-time values scales with how isolated a linear chain of nodes is and that the presence of chain motifs is related to extreme hitting-time values even in random networks with mixed topologies above and beyond modularity of the network. Resting brain networks also have extreme hitting times that are likely related to hierarchical processing in sensory cortex. When they are most isolated from the rest of the network, hierarchical processing streams resemble the chain of nodes on the linear component of a lollipop graph. This parallel motivates the use of extremely long random walks between brain areas as a measure of the presence, and relative isolation, of hierarchical processing streams. In particular, hitting time of a region of interest can be utilized to detect presence of linear components likely to be hierarchical processing streams. A central dogma of neuroscience is that sensory representations are constructed hierarchically (Hubel & Wiese, 1962; Kikuchi, Horwitz, & Mishkin, 2010; Van Essen & Maunsell, 1983). Hierarchical processing streams have also been a focal component of computer vision models since 1971 (Giebel, 1971) and a significant contributor to the success of modern convolutional neural networks (LeCun, Bengio, & Hinton, 2015). Their foundational nature has made the study of hierarchical processing streams the focus of targeted analyses (e.g., Sepulcre, Sabuncu, Yeo, Liu, & Johnson, 2012). Here, we showed that nodes from sensory and motor areas of the brain have extreme hitting times that contribute to Kelley skewness. By comparing resting to task-based network topologies, we can show that decreases in hitting time are also associated with sensory hierarchies becoming less chain like.

Task changes in functional connectivity can be observed as changes in functional brain network topology. Previous work has highlighted the central role of path length and the integration of isolated paths in function. In Goñi et al. (2014), a notion of path transitivity — which accounted for not only the shortest path, but also local detours along that path — was the best predictor of functional connectivity. Similar notions of distributed communicability (related to the diffusion of information over the network) were used to quantify the disruption of the global communication in the cortex that was triggered by the pharmacogenetic inactivation of the amygdala (Grayson et al., 2016), and to detect changes in functional connectivity after a stroke (Crofts et al., 2011). A thorough review of these concepts and their relationships to the notion of mean first-passage time, which is equivalent to the mean hitting time, is provided in Avena-Koenigsberger et al. (2017). Because the mean hitting time conflates overall changes in connectivity with changes to a subnetwork, these changes may be better explained using Kelley skewness, which specifically focuses on extreme values and so provides a mechanism to identify potential subnetwork changes. Extreme values contributing to connectivity skewness were associated with sensory areas of the brain specifically associated with the task. Hitting times in these sensory areas of the brain became shorter and less extreme during BART task performance. Sensory areas became more strongly connected to distant areas throughout the brain. The nodes with the largest reductions in hitting time were found in brain sensory areas related to the BART task (somatosensory and visual areas). One additional area also showed a decrease in hitting time: PF. PF is located in the inferior parietal lobule and is thought to be related to risk processing (Weber & Huettel, 2008). In line with its role in the processing of visual magnitude, it showed increased connectivity with visual inputs. Broadly, the introduction of a task caused sensory processing streams to become better connected to other task-relevant areas, and less chain-like. This result is somewhat counterintuitive since hierarchical processing pipelines are often described as most distinct when active. We do find evidence of increased connectivity within sensory networks, but these increases in strength within the sensory processing stream are offset by wider integration, making their network topology less chain-like. In addition, whether the processing pipeline becomes more or less integrated depends on the calculation underlying the transition probability between areas. When similar models are



constructed using the raw correlation values, group and task differences in the same dataset are consistent but in the opposite direction (Rezaeinia & Carter, 2017). This is likely due to the redundant connections and task event correlations (Cole et al., 2018) included in raw correlation models. Here, we focused on the partial correlation of brain region time series that minimizes redundant connections, following the state of the art in the field (Smith et al., 2011). In spite of the complexities raised, the distribution of task-relevant information throughout the brain is consistent with what would be most likely to improve BART task performance and supports the interpretation of sensory hierarchies as existing as relatively isolated linear network topologies during rest. In future work it would be helpful to incorporate additional multifaceted tasks to generalize these findings to the incorporation of sensory information under other constraints.

Skewness of the connectivity distribution also explains cortical network differences between psychiatric diagnoses. Resting functional connectivity in a large neurotypical population is significantly positively skewed. In such a case, average efficiency for such a network would be biased and less representative of the network as a whole. An important finding is that changes in connectivity between clinical and control populations are due to changes in skewness rather than average differences. In fact, the median of connectivity measures changed in the opposite direction with respect to the average. Network connectivity changes between clinical and control populations are therefore due to a subset of connections rather than the network as a whole. The identification of specific cortical regions involved in topological changes between neurotypical and clinical populations provides an opportunity to better understand functional changes that occur in those populations as well as opportunities for improving diagnosis. Task performance reduced hitting-time skewness by increasing the connectivity between sensory areas and the rest of the cortical network. Qualitatively similar changes are seen in clinical populations, implying further work exploring network topology changes to specific tasks may help characterize the atypical resting connectivity for individuals with a schizophrenia or bipolar diagnosis. A testable prediction from this implied mechanistic difference would be that individuals with these diagnoses spend less time in activities typically associated with resting fMRI (e.g., future planning).

The results presented were based on theoretical predictions and applied to a publicly available dataset in a rigorous manner. We would like to document the following caveats and qualifications. First, although linear components in networks produce maximal hitting times in theory, it is possible that other network topologies could also produce some degree of skewness. To answer this concern, we showed that in toy examples skewness was related to short linear graphs or linear graphs that were still connected to the rest of the graph. We also found that the hitting-time distribution of both small-world, lollipop, and random graphs are skewed but that skewness in both cases is dominated by linear paths, even with a linear path that comprises significantly less than a third of the graph. It is, however, important to note that the number of linear topologies does not explain all of the variance in Kelley skewness and so there could be other contributing topologies, perhaps related to modularity and degree. In our human fMRI analyses, the network as a whole did not become less connected (see the Supporting Information), and those areas with extreme values become less chain-like when they have smaller hitting times. Thus, the relationship between extreme hitting times and linear paths is robust. In addition, past work on sensory hierarchies (Hubel & Wiesel, 1962; Kikuchi et al., 2010; Van Essen & Maunsell, 1983), recent work showing parallels between convolutional neural networks and sensory networks (Güçlü & van Gerven, 2015; Kell, Yamins, Shook, Norman-Haignere, & McDermott, 2018; Khaligh-Razavi & Kriegeskorte, 2014), and the integration of sensory networks during task performance (see above) are all consistent with the presence of linear components in the cortical network. Second, we focused on a cortical model of brain

function, and the absence of subcortical nodes could have affected the topology of the network model. However, the inclusion of subcortical connections to cortical network end points should not change connectivity measures since the path would still produce larger hitting times (the largest times may then be shifted to the middle of the sensory hierarchy).

### CONCLUSION

In conclusion, establishing a link between network topologies, hierarchical processing pipelines, task engagement, and psychiatric disorders provides an opportunity to interpret cortical network changes in the light of cognitive models of brain function. The interpretation of network connectivity and information processing topologies is an area of significant focus for neuroscience (Fornito & Bullmore, 2015). The widespread collection of rfMRI in particular provides a unique opportunity to extend this work to numerous psychiatric disorders and compare these findings with the growing body of open-source fMRI task data.

### ACKNOWLEDGMENTS

Publication of this article was funded by the University of Colorado Boulder Libraries Open Access Fund. The research was supported by the Department of Electrical and Computer Engineering, University of California San Diego, and Department of Electrical, Computer, and Energy Engineering and Institute of Cognitive Science of the University of Colorado Boulder. Piya Pal was supported in part by NSF NCS-FO 1734940 and UC San Diego. We would like to acknowledge members of Social Neuroscience and Games (SNaG) Lab, and Psychology and Neuroscience Department at the University of Colorado Boulder whose comments helped us improve our work. We would like to especially thank Heejung Jung, John Pearson, Terry Sejnowski, and David Smith for manuscript review during its preparation.

### SUPPORTING INFORMATION

Supporting information for this article is available at [https://doi.org/10.1162/netn\\_a\\_00122](https://doi.org/10.1162/netn_a_00122). Code for analysis in this project can be found under the first author's name on GitHub: [https://github.com/SNaGLab/Rezaeinia\\_et\\_al\\_Hitting\\_time\\_analysis](https://github.com/SNaGLab/Rezaeinia_et_al_Hitting_time_analysis) (Rezaeinia, 2018).

### AUTHOR CONTRIBUTIONS

Paria Rezaeinia: Conceptualization; Data curation; Formal analysis; Investigation; Methodology; Resources; Software; Validation; Visualization; Writing - Original Draft; Writing - Review & Editing. Kim Fairley: Formal analysis; Writing - Review & Editing. Piya Pal: Methodology; Supervision; Writing - Review & Editing. François G. Meyer: Conceptualization; Methodology; Supervision; Writing - Review & Editing. R. McKell Carter: Conceptualization; Formal analysis; Investigation; Methodology; Project administration; Software; Supervision; Visualization; Writing - Original Draft; Writing - Review & Editing.

### FUNDING INFORMATION

Piya Pal, National Science Foundation (<http://dx.doi.org/10.13039/100000001>), Award ID: 1734940. University of Colorado Boulder Libraries Open Access Fund.

### REFERENCES

Achard, S., & Bullmore, E. (2007). Efficiency and cost of economical brain functional networks. *PLoS Computational Biology*, 3(2), e17.

Aldous, D., & Fill, J. (2002). Reversible Markov chains and random walks on graphs [Unfinished monograph]. Retrieved from <https://www.stat.berkeley.edu/~aldous/RWG/book.html>

- Avena-Koenigsberger, A., Masic, B., & Sporns, O. (2017). Communication dynamics in complex brain networks. *Nature Reviews Neuroscience*, *19*, 17–33. <https://doi.org/10.1038/nrn.2017.149>
- Bassett, D. S., & Sporns, O. (2017). Network neuroscience. *Nature Neuroscience*, *20*, 353–364. <https://doi.org/10.1038/nn.4502>
- Besnard, J. L., Bassett, D. S., Smallwood, J., Margulies, D. S., Derntl, B., Gruber, O., . . . Bzdok, D. (2018). Different shades of default mode disturbance in schizophrenia: Subnodal covariance estimation in structure and function. *Human Brain Mapping*, *39*(2), 644–661. <https://doi.org/10.1002/hbm.23870>
- Brightwell, G., & Winkler, P. (1990). Maximum hitting time for random walks on graphs. *Random Structures and Algorithms*, *1*(3), 263–276. <https://doi.org/10.1002/rsa.3240010303>
- Bullmore, E., & Sporns, O. (2009). Complex brain networks: Graph theoretical analysis of structural and functional systems. *Nature Reviews Neuroscience*, *10*(3), 186.
- Bullmore, E. T., & Bassett, D. S. (2011). Brain graphs: Graphical models of the human brain connectome. *Annual Review of Clinical Psychology*, *7*(1), 113–140. <https://doi.org/10.1146/annurev-clinpsy-040510-143934>
- Cheng, W., Rolls, E., Zhang, J., Sheng, W., Ma, L., Wan, L., . . . Feng, J. (2016). Functional connectivity decreases in autism in emotion, self, and face circuits identified by knowledge-based enrichment analysis. *NeuroImage*, *148*.
- Cherniak, C. (1990). The bounded brain: Toward quantitative neuroanatomy. *Journal of Cognitive Neuroscience*, *2*(1), 58–68.
- Cole, M. W., Ito, T., Schultz, D., Mill, R., Chen, R., & Cocuzza, C. (2018). Task activations produce spurious but systematic inflation of task functional connectivity estimates. *bioRxiv*. <https://doi.org/10.1101/292045>
- Crofts, J. J., Higham, D. J., Bosnell, R., Jbabdi, S., Matthews, P. M., Behrens, T. E. J., & Johansen-Berh, H. (2011). Network analysis detects changes in the contralesional hemisphere following stroke. *NeuroImage*, *54*(1), 161–169. <https://doi.org/10.1016/j.neuroimage.2010.08.032>
- Dennis, E. L., & Thompson, P. M. (2014). Functional brain connectivity using fMRI in aging and Alzheimer's disease. *Neuropsychology Review*, *24*(1), 49–62. <https://doi.org/10.1007/s11065-014-9249-6>
- Erdős, P., & Rényi, A. (1959). On random graphs I. *Publicationes Mathematicae (Debrecen)*, *6*, 290–297.
- Essen, D. C. V., Smith, S. M., Barch, D. M., Behrens, T. E., Yacoub, E., & Ugurbil, K. (2013). The WU-MINN Human Connectome Project: An overview. *NeuroImage*, *80*, 62–79. <https://doi.org/10.1016/j.neuroimage.2013.05.041>
- Fornito, A., (2016). Graph theoretic analysis of human brain networks. M. Filippi (Eds.). *fMRI techniques and protocols* (pp. 283–314). New York, NY: Springer New York. [https://doi.org/10.1007/978-1-4939-5611-1\\_10](https://doi.org/10.1007/978-1-4939-5611-1_10)
- Fornito, A., & Bullmore, E. T. (2015). Reconciling abnormalities of brain network structure and function in schizophrenia. *Current Opinion in Neurobiology*, *30*, 44–50.
- Fox, M. D., & Greicius, M. (2010). Clinical applications of resting state functional connectivity. *Frontiers in Systems Neuroscience*, *4*, 19.
- Friston, K. (2010). The free-energy principle: A unified brain theory? *Nature Reviews Neuroscience*, *11*(2), 12–138.
- Giebel, H. (1971). Feature extraction and recognition of hand-written characters by homogeneous layers. In O.-J. Grüsser & R. Klinke (Eds.), *Zeichenerkennung durch biologische und technische systeme / Pattern recognition in biological and technical systems* (pp. 162–169). Berlin, Germany: Springer Berlin Heidelberg.
- Glasser, M. F., Coalson, T. S., Robinson, E. C., Hacker, C. D., Harwell, J., Yacoub, E., . . . Van Essen, D. C. (2016). A multi-modal parcellation of human cerebral cortex. *Nature*, *536*, 171–178. <https://doi.org/10.1038/nature18933>
- Goñi, J., Avena-Koenigsberger, A., Velez de Mendizabal, N., van den Heuvel, M. P., Betzel, R. F., & Sporns, O. (2013). Exploring the morphospace of communication efficiency in complex networks. *PLS ONE*, *8*(3), 1–10. <https://doi.org/10.1371/journal.pone.0058070>
- Goñi, J., van den Heuvel, M. P., Avena-Koenigsberger, A., Velez de Mendizabal, N., Betzel, R. F., Griffa, A., . . . Sporns, O. (2014). Resting-brain functional connectivity predicted by analytic measures of network communication. *Proceedings of the National Academy of Sciences*, *111*(2), 833–838. <https://doi.org/10.1073/pnas.1315529111>
- Goulas, A., Schaefer, A., & Margulies, D. S. (2015). The strength of weak connections in the macaque cortico-cortical network. *Brain Structure and Function*, *220*(5), 2939–2951. <https://doi.org/10.1007/s00429-014-0836-3>
- Grayson, D. S., Bliss-Moreau, E., Machado, C. J., Bennett, J., Shen, K., Grant, K. A., . . . Amaral, D. G. (2016). The rhesus monkey connectome predicts disrupted functional networks resulting from pharmacogenetic inactivation of the amygdala. *Neuron*, *91*(2), 453–466. <https://doi.org/10.1016/j.neuron.2016.06.005>
- Greicius, M. D., Krasnow, B., Reiss, A. L., & Menon, V. (2003). Functional connectivity in the resting brain: A network analysis of the default mode hypothesis. *Proceedings of the National Academy of Sciences*, *100*(1), 253–258. <https://doi.org/10.1073/pnas.0135058100>
- Güçlü, U., & van Gerven, M. A. J. (2015). Deep neural networks reveal a gradient in the complexity of neural representations across the ventral stream. *Journal of Neuroscience*, *35*(27), 10005–10014. <https://doi.org/10.1523/JNEUROSCI.5023-14.2015>
- Hubel, D. H., & Wiesel, T. N. (1962). Receptive fields, binocular interaction and functional architecture in the cat's visual cortex. *Journal of Physiology*, *160*, 106–154.
- Kell, A. J. E., Yamins, D. L. K., Shook, E. N., Norman-Haignere, S. V., & McDermott, J. H. (2018). A task-optimized neural network replicates human auditory behavior, predicts brain responses, and reveals a cortical processing hierarchy. *Neuron*, *98*(3), 630–644. <https://doi.org/10.1016/j.neuron.2018.03.044>
- Kelley, T. L. (1923). *Statistical method*. New York, NY: Macmillan Company.
- Khaligh-Razavi, S.-M., & Kriegeskorte, N. (2014). Deep supervised, but not unsupervised, models may explain cortical representation. *PLS Computational Biology*, *10*(11), 1–29. <https://doi.org/10.1371/journal.pcbi.1003915>
- Khambhati, A. N., Medaglia, J. D., Karuza, E. A., Thompson-Schill, S. L., & Bassett, D. S. (2018). Subgraphs of functional brain networks identify dynamical constraints of cognitive control. *PLS Computational Biology*, *14*(7), 1–33. <https://doi.org/10.1371/journal.pcbi.1006234>

- Kikuchi, Y., Horwitz, B., & Mishkin, M. (2010). Hierarchical auditory processing directed rostrally along the monkey's supra-temporal plane. *Journal of Neuroscience*, *30*(39), 13021–13030. <https://doi.org/10.1523/JNEUROSCI.2267-10.2010>
- Lambiotte, R., Delvenne, J., & Barahona, M. (2014). Random Walks, Markov Processes and the multiscale modular organization of complex networks. *IEEE Transactions on Network Science and Engineering*, *1*(2), 76–90. <https://doi.org/10.1109/TNSE.2015.2391998>
- Latora, V., & Marchiori, M. (2001). Efficient behavior of small-world networks. *Physical Review Letters*, *87*, 198701. <https://doi.org/10.1103/PhysRevLett.87.198701>
- LeCun, Y., Bengio, Y., & Hinton, G. (2015). Deep learning. *Nature*, *521*, 436–444. <https://doi.org/10.1038/nature14539>
- Li, P., Fan, T.-T., Zhao, R.-J., Han, Y., Shi, L., Sun, H.-Q., . . . Lu, L. (2017). Altered brain network connectivity as a potential endophenotype of schizophrenia. *Scientific Reports*, *7*(1), 5483. <https://doi.org/10.1038/s41598-017-05774-3>
- Lovász, L., & Simonovits, M. (1993). Random walks in a convex body and an improved volume algorithm. *Random Structures and Algorithms*, *4*(4), 359–412. <https://doi.org/10.1002/rsa.3240040402>
- Newman, M.E.J., & Girvan, M. (2004). Finding and evaluating community structure in networks. *Physical Review E*, *69*, 026113. <https://doi.org/10.1103/PhysRevE.69.026113>
- Norris, J. R. (1997). *Markov chains*. Cambridge, United Kingdom: Cambridge University Press. <https://doi.org/10.1017/CBO9780511810633>
- Poldrack, R., Congdon, E., Triplett, W., Gorgolewski, K., Karlsgodt, K., Mumford, J., . . . Bilder, R. (2016). A phenome-wide examination of neural and cognitive function. *bioRxiv*. <https://doi.org/10.1101/059733>
- Raichle, M. E., MacLeod, A. M., Snyder, A. Z., Powers, W. J., Gusnard, D. A., & Shulman, G. L. (2001). A default mode of brain function. *Proceedings of the National Academy of Sciences*, *98*(2), 676–682. <https://doi.org/10.1073/pnas.98.2.676>
- Reijneveld, J. C., Ponten, S. C., Berendse, H. W., & Stam, C. J. (2007). The application of graph theoretical analysis to complex networks in the brain. *Clinical Neurophysiology*, *118*(11), 2317–2331. <https://doi.org/10.1016/j.clinph.2007.08.010>
- Rezaeinia, P. (2018). Hitting time analysis for brain networks, GitHub. [https://github.com/SNaGLab/Rezaeinia\\_et\\_al\\_Hitting\\_time\\_analysis](https://github.com/SNaGLab/Rezaeinia_et_al_Hitting_time_analysis)
- Rezaeinia, P., & Carter, R. M. (2017). Using hitting-time interdecile differences to identify brain networks with path-like features. Rubinov, M., & Sporns, O. (2011). Weight-conserving characterization of complex functional brain networks. *NeuroImage*, *56*(4), 2068–2079. <https://doi.org/10.1016/j.neuroimage.2011.03.069>
- Sepulcre, J., Sabuncu, M. R., Yeo, T. B., Liu, H., & Johnson, K. A. (2012). Stepwise connectivity of the modal cortex reveals the multimodal organization of the human brain. *Journal of Neuroscience*, *32*(31), 10649–10661. <https://doi.org/10.1523/JNEUROSCI.0759-12.2012>
- Shen, X., & Meyer, F. (2008). Low dimensional embedding of fMRI datasets. *NeuroImage*, *41*, 886–902.
- Smith, S. M., Fox, P. T., Miller, K. L., Glahn, D. C., Fox, P. M., Mackay, C. E., . . . Beckmann, C. F. (2009). Correspondence of the brain's functional architecture during activation and rest. *Proceedings of the National Academy of Sciences*, *106*(31), 13040–13045. <https://doi.org/10.1073/pnas.0905267106>
- Smith, S. M., Miller, K. L., Salimi-Khorshidi, G., Webster, M., Beckmann, C. F., Nichols, T. E., . . . Woolrich, M. W. (2011). Network modelling methods for fmri. *NeuroImage*, *54*(2), 875–891. <https://doi.org/10.1016/j.neuroimage.2010.08.063>
- Stiso, J., & Bassett, D. S. (2018). Spatial embedding imposes constraints on neuronal network architectures. *Trends in Cognitive Sciences*, *22*(12), 1127–1142. <https://doi.org/10.1016/j.tics.2018.09.007>
- Trujillo-Ortiz, A., & Hernandez-Walls, R. (2003). DagosPtest, MATLAB Central File Exchange.
- van den Heuvel, M. P., & Pol, H. E. H. (2010). Exploring the brain network: A review on resting-state fMRI functional connectivity. *European Neuropsychopharmacology*, *20*(8), 519–534. <https://doi.org/10.1016/j.euroneuro.2010.03.008>
- Van Essen, D. C., & Maunsell, J. H. R. (1983). Hierarchical organization and functional streams in the visual cortex. *Trends in Neurosciences*, *6*, 370–375.
- Watts, D. J., & Strogatz, S. H. (1998). Collective dynamics of “small-world” networks. *Nature*, *393*, 440. <https://doi.org/10.1038/30918>
- Weber, B. J., & Huettel, S. A. (2008). The neural substrates of probabilistic and intertemporal decision making. *Brain Research*, *1234*, 104–115. <https://doi.org/10.1016/j.brainres.2008.07.105>
- Zalesky, A., Fornito, A., & Bullmore, E. T. (2010). Network-based statistic: Identifying differences in brain networks. *NeuroImage*, *53*(4), 1197–1207. <https://doi.org/10.1016/j.neuroimage.2010.06.041>